Bow Echoes: A Tribute to T. T. Fujita

Morris L. Weisman
National Center for Atmospheric Research,* Boulder, Colorado

ABSTRACT

Bow echoes represent one of the unique and more well-known forms of severe convective organization, often being responsible for the production of long swaths of damaging surface winds and small tornadoes. They are identified by their characteristic bow shape as seen on radar reflectivity displays. Much of what is known about bow echoes originated with T. T. Fujita, whose observational insights and careful analyses two decades ago still guide research and forecasting of bow-echo phenomena today. This paper reviews Fujita's contributions to our understanding of bow echoes, and also summarizes more recent observational and numerical studies that have built on the foundation that he provided. Perhaps not surprisingly, the life cycle of bow echoes as first described by Fujita, consisting of an evolution from a symmetric line of convective cells to a comma-shaped echo with a dominant cyclonic vortex, is now recognized as one of the fundamental modes of mesoconvective evolution, for both severe and nonsevere convective systems alike.

1. Introduction

On the early morning of 15 July 1995, a convective system spawned over Ontario and moved across much of upper New York State and central New England, producing surface winds of 30 to over 45 m s^{-1} (60 to over 90 kt), killing eight people, and producing one of the largest tree blowdowns ever observed in the Adirondack Mountains (Cannon et al. 1998; McCarthy 1996; Bosart et al. 1998). On 5 May 1996, a convective system moved rapidly across the lower Ohio Valley, producing wind gusts up to 41 m s^{-1} and widespread wind damage over much of eastern Missouri, southern Illinois, and northern Kentucky (Spoden et al. 1998). On the night of 16 May and early on the morning of 17 May 1996, a convective system raced across South Dakota, producing straight-line winds in excess of 50 m s^{-1} (100 kt), toppling nearly 600 power poles and producing widespread damage to buildings (Rasch and van Ess 1998).

Long-lived, convectively produced windstorms, such as those mentioned above, pose a significant hazard to life and property over much of the United States during the spring and summer months. These events have been given a generic name of derecho (Johns and Hirt 1987), a term that originated in the late 1800s to refer to convective systems producing wide and long swaths of straight-line wind damage (Hinrichs 1888). More detailed studies of these events, however, have shown that a vast majority are associated with a particular type of organized convective system, which is more popularily referred to as a bow echo (so named due to its characteristic bow shape on radar displays). First named and described in detail by Fujita (1978), bow echoes now represent

Morris L. Weisman

*The National Center for Atmospheric Research is sponsored by the National Science Foundation.

Corresponding author address: Dr. Morris L. Weisman, National Center for Atmospheric Research, Boulder, CO 80307.
E-mail: weisman@ucar.edu

In final form 22 June 2000.

one of the best-known modes of convective organization associated with severe weather events, especially for high winds.

The goal of this paper is to review Fujita's contributions to our current recognition and understanding of bow-echo phenomena, and to summarize the subsequent progress that we have made in understanding and forecasting such events. Only in the last few years have we fully recognized the significance of his initial analyses and diagnostic insights. The basic structure that he first described for bow echoes back in 1978 is now recognized as one of the primary modes of mesoconvective organization, for severe and nonsevere systems alike.

2. The origin of the bow echo

Fujita's interest in bow echoes originated from his more general interest in identifying convective structures and precursors associated with downbursts and microbursts. A complementary paper describing his contributions to understanding downbursts is also included in this volume (Wilson and Wakimoto 2001). In preparation for the Northern Illinois Meteorological Research on Downbursts (NIMROD) project (Fujita 1978), he identified two particular radar cell types as especially significant for the production of downburst phenomena: the hook echo, which was already well associated with supercell storms and tornadoes, and a bow-shaped line of cells, which we now commonly refer to as a bow echo (Fig. 1).

The significance of bow-shaped systems of convective cells did not originate with Fujita; it was first noted by Nolen (1959), who identified an association between a line-echo-wave pattern (LEWP) in radar reflectivity and the occurrence of tornadoes. Hamilton (1970) further emphasized the significance of LEWPs by identifying the association of this feature with damaging straight-line winds, as well as tornadoes. Through many case studies, Fujita went well beyond the previous investigators and proposed a kinematic structure and a characteristic evolution for such systems. He emphasized that one of the distinct characteristics of bow echoes was their tendency to produce very long swaths of damaging straight-line winds. He also recognized that these bow echoes could occur either individually or as part of a LEWP.

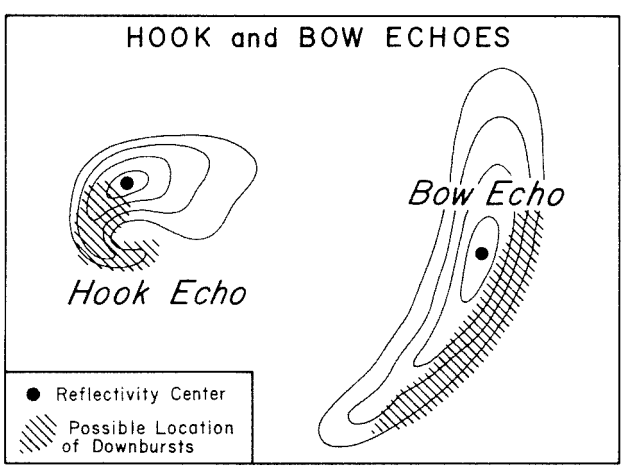

FIG. 1. Hook and bow echoes commonly observed during downbursts. [From Fujita (1978).]

A typical morphology of radar echoes associated with a bow echo, as envisioned by Fujita (1978; referred to as a downburst in this reference), is presented in Fig. 2. The system usually begins as a single, large, and strong convective cell that may be either isolated or part of a more extensive squall line. As the strong surface winds develop, the initial cell evolves into a bow-shaped line segment of cells, with the strongest winds occurring at the apex of the bow. During its most intense phase (Fig. 2c), the center of the bow may form a spearhead echo (e.g., Fujita and Byers 1977). During the declining stage, the system often evolves into a comma-shaped echo (Fig. 2e).

An example is presented in Fig. 3 for a case that occurred on 4 July 1977 in northern Wisconsin. This particular bow echo had a scale of 80–100 km as it evolved through the above-described life cycle over a 6-h period. The path of strong, damaging surface winds, although narrower than that for the full convective system, is almost continuous through the lifetime of the system. Peak wind gusts over 52 m s^{-1} (115 mph) were recorded with its passage, with F1–F2 damage on the Fujita scale (Fujita 1981) scattered all along the system's path. A more detailed analysis of the wind damage is presented in Fig. 4, clearly indicating that a wide range of scales can be associated with such events, with smaller-scale microbursts and downbursts embedded within a more general mesoscale swath of strong winds. No evidence of a tornado was found anywhere within this downburst swath. As with most of Fujita's studies, the degree of care and detail put into these analyses is quite remarkable and has rarely been equaled since.

One of the key attributes noted in Fujita's conceptual model (Fig. 2) is the unique mesoscale flow features associated with the ends of the bowing segments. Fujita (1978) states, "Both cyclonic and anticyclonic

motions of small echoes are seen near the ends of the bow. Although the anticyclonic motion does not amplify with time, cyclonic rotation on the left side often turns into a rotating head." Although Doppler radar data were not generally available at this time, Fujita was able to deduce this flow configuration by careful analysis of the motions of small cells relative to the stronger bow echo. An example of such an analysis is depicted in Fig. 5 for the 4 July 1977 case described above. Interestingly, this methodology for deducing winds from small echo motions has recently become an established analysis technique for deducing mesoscale motions, using clear-air boundary layer features as well as using echo returns from weak precipitation features [e.g., tracking radar echoes by correlation; Rhinehart and Garvey (1978) and Tuttle and Foote (1990)]. However, while these more recent techniques are based on automated computer algorithms, Fujita's analyses were all done by hand. Fujita's deductions concerning the flow field in bow echoes were quickly verified once Doppler observations became available.

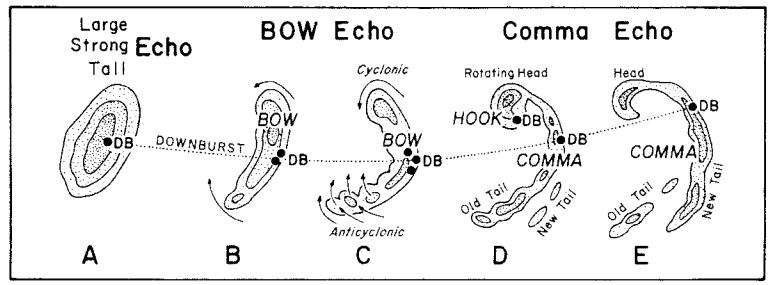

FIG. 2. A typical morphology of radar echoes associated with bow echoes that produce strong and extensive downbursts, labeled DB. [From Fujita (1978).]

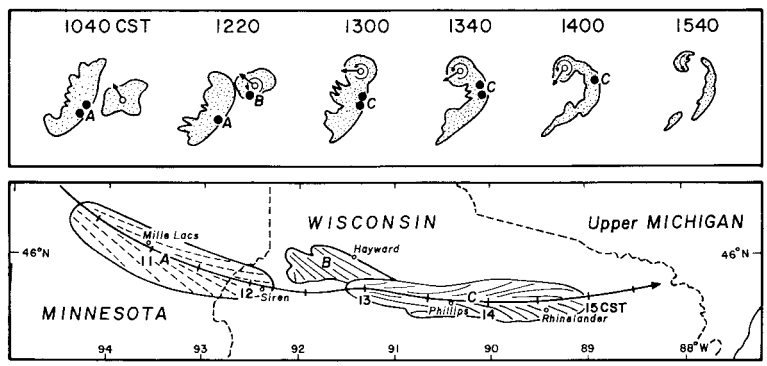

FIG. 3. Evolution of a bow echo into a comma echo during the 4 Jul 1977 downbursts in northern Wisconsin. Downbursts A and C were associated with a bow echo while B was associated with a hook echo. Motion of the hook echo is relative to the bow echo. No tornado was associated with this storm. [From Fujita (1978).]

Fujita (1978) hypothesized that, in association with the damaging downburst winds, there must also be a strong rear-inflow jet, with its core at the apex of the bow. Such a rear-inflow feature is depicted in a vertical cross section derived for the 4 July bow echo in Fig. 6. At the onset of a strong downburst, the midlevel flow accelerates into the convection from the rear. As a result, the convective cells propagate more

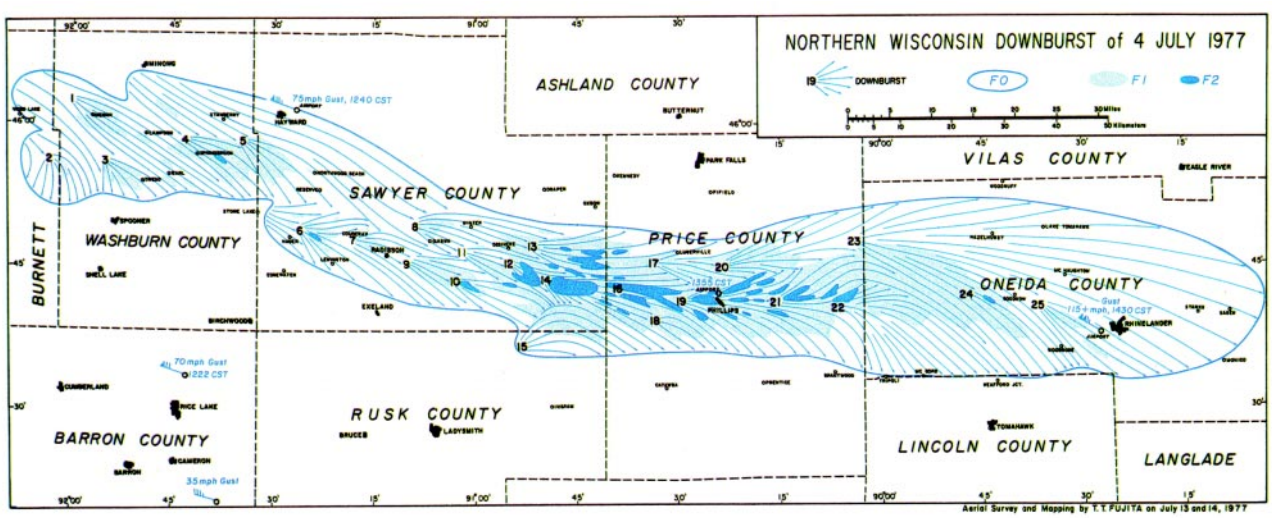

FIG. 4. Twenty-five downbursts on Independence Day in northern Wisconsin left behind a damage swath 166 mi long and 17 mi wide. No evidence of a tornado was found anywhere. [From Fujita (1978).]

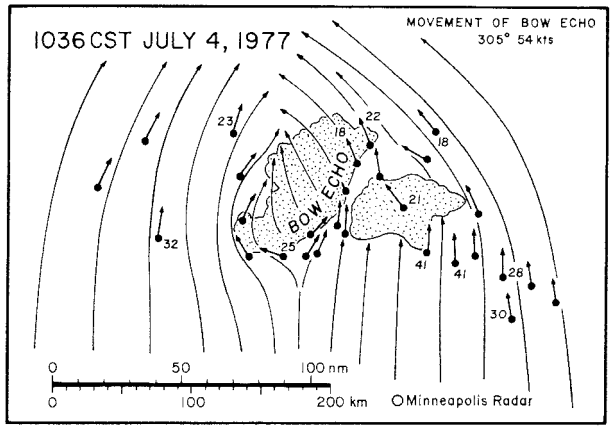

FIG. 5. Relative motion of echoes with respect to the northern Wisconsin bow echo at 1036 CST 4 Jul 1977 (from Fujita 1978).

quickly at the core of the system, helping to create the bow shape.

Another common characteristic of bow echoes is documented in Fig. 7 for a storm that passed through Springfield, Illinois, on 6 August 1977. This system evolved from a relatively isolated cell to a comma-shaped echo over a 5-h period while producing a continuous swath of damaging surface winds. In this particular case, 18 tornadoes were generated just to the north of the bow echo apex as the northernmost cell evolved into a cyclonically rotating head. The relationship between bow echoes and tornadoes has still not been adequately explained. Figure 8 again illustrates the degree of care and detail Fujita put into his analysis of the surface wind features associated with the 6 August system, showing in unprecedented detail the relationship between the tornadoes and downbursts. Further analysis of this case is presented in Forbes and Wakimoto (1983).

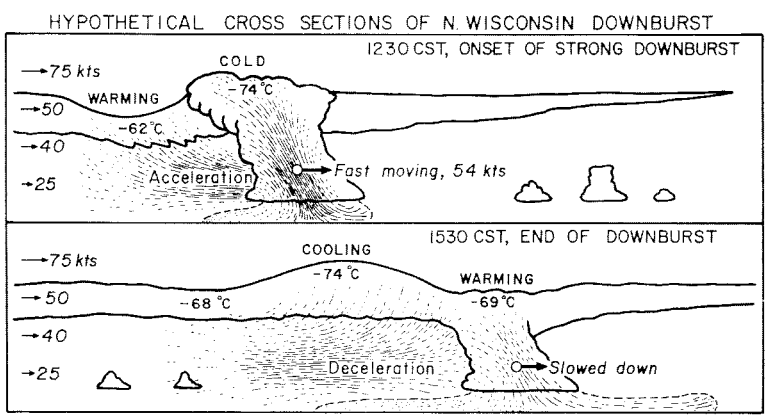

FIG. 6. Hypothetical cross sections of northern Wisconsin downburst at 1230 and 1530 CST 4 Jul 1977. [From Fujita (1978).]

Fujita was known for using every tool at his disposal to understand the phenomena that he was researching. Along these lines, Fujita also explored the potential for using satellite data to both monitor and interpret bow echoes. He was especially interested in identifying features on satellite pictures that could provide clues to a forecaster as to the existence of strong downburst winds at the surface. One such feature that he identified was a relatively warm region on the IR images that appeared just upwind of the comma head of a mature bow echo, as shown in Fig. 9 for the 4 July 1977 case and the Springfield case presented above. This warming could be interpreted as an area of mesoscale descent in the upper troposphere associated with the downburst winds below, as also depicted in the vertical cross section in Fig. 6 for the 4 July case. To this author's knowledge, however, there have been no further studies considering the significance and usefulness of such observations.

When proposing conceptual models, Fujita was always very careful to discuss the potential limitations to his analyses. For instance, in reference to the vertical cross section proposed in Fig. 6, which was constructed based on both radar and the satellite observations described above, he states (Fujita 1978): "Hypothetical cross sections and a conceptual model in Figures 6.12 and 6.13 [Fig. 6.12 is repeated here as Fig. 6] are introduced in an attempt to explain characteristics of both satellite and radar imagery. No attempt has been made to offer alternative explanations of the analytical results. More cases of extensive downburst families are necessary in order to understand this phenomenon better." To Fujita, getting research results out quickly to stimulate community interest seemed paramount. Final answers would follow over time.

With the advent of Project NIMROD in 1978 (Fujita 1979) came Fujita's first opportunity to observe downburst and bow-echo phenomena with Doppler radar. He took advantage of this opportunity on 25 June 1978 when he produced a dual-Doppler analysis of a bow-echo event using hand-drawn vectors derived from the radial winds (Fig. 10). His interpretation of this analysis forced him to rethink the cause and effect relationship between bow echoes and downburst winds (Fujita 1979): "Prior to the NIMROD operation, Fujita (1978) called the bulged echo the 'bow echo,' identifying its final stage as

the 'comma echo.' In these studies, a bulge of echo was regarded as an 'inducer of high wind.' The preliminary research of NIMROD data is going to reverse this 'chicken and egg' relationship. Fujita's 1979 model of bow-echo evolution highlights the downburst as the cause of the bulge or the bow. The model in Figure 6 [see Fig. 11] shows that the bow is caused by the downburst instead. Namely, a downburst is already in progress when a line echo takes the shape of a bow."

Fujita (1979) further conjectures: "The downburst airflow associated with a bow echo is most likely to be the result of a snowballing collapse of a majestic thunderstorm. Apparently, an overgrown thunderstorm suddenly reverses its airflow direction upside-down, upon reaching a critical point of no return."

As will be presented later, recent studies suggest that both conceptual models are essentially correct: a strong downdraft and resultant strong surface cold pool is critical for the initial development of bow echoes, but the mesoscale wind features thereby produced can further enhance the intensity and longevity of the severe wind event. His further suggestion that bow echoes necessarily result from a collapsing thunderstorm, however, has not generally been supported by more recent studies.

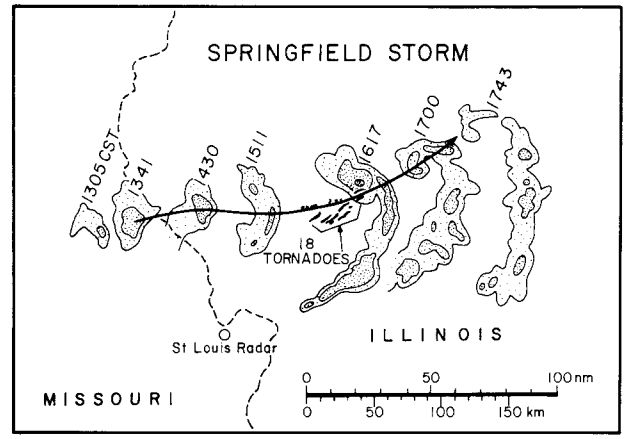

FIG. 7. Evolution of radar echoes associated with Springfield downbursts and tornadoes of 6 Aug 1977. [From Fujita (1978).]

Fujita was quite successful at identifying the key structural and evolutionary characteristics of bow echoes. However, the lack of a Doppler radar network along with other mesoscale data sources at the time made it very difficult to confirm many of the kinematical features that he inferred. Thus, any attempt to explain the mesoscale flow features such as the rear-inflow jet or rotational features would have been

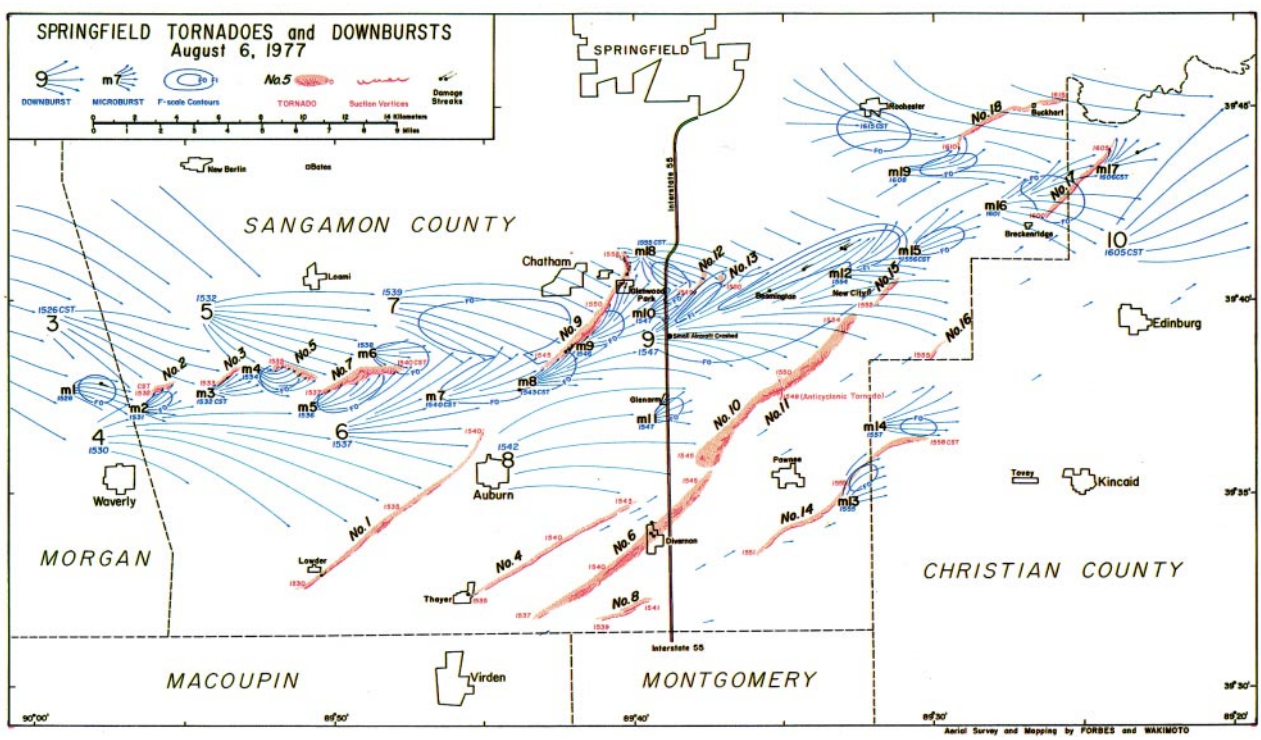

FIG. 8. Eighteen tornadoes, 10 downbursts, and 17 microbursts are depicted in this map. One tornado (no. 11) was anticyclonic. Apparently, eight tornadoes formed on the left side of microbursts. No traces of downbursts were found in the vicinity of other tornadoes. [From Fujita (1978).]

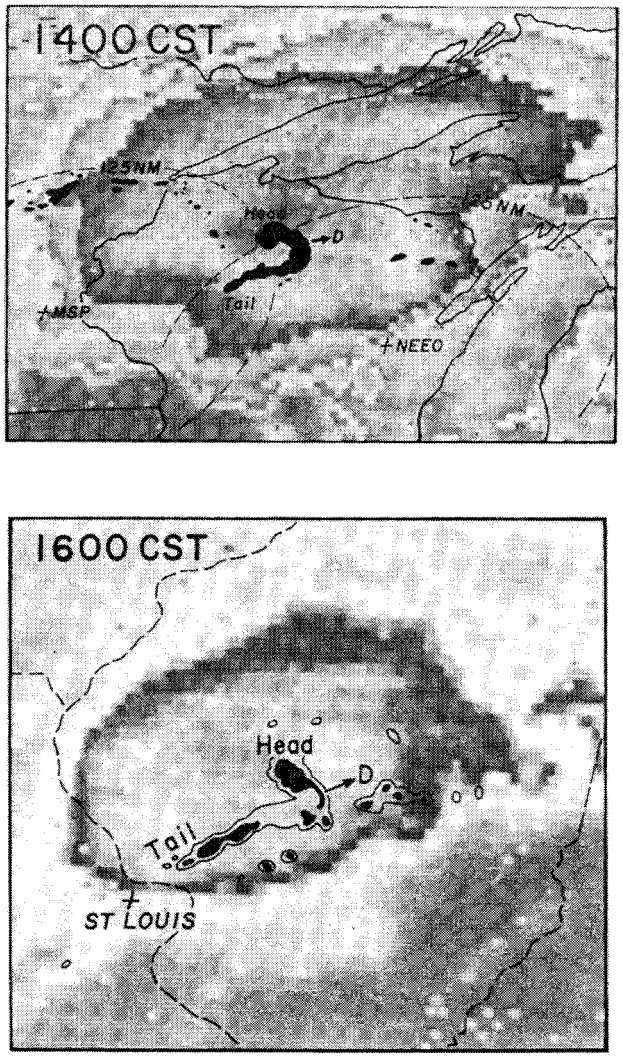

FIG. 9. Infrared cloud-top temperatures with radar echoes for (a) the Springfield downburst at 1600 CST and (b) the 4 Jul 1977 bow echo at 1400 CST. In both cases, a region of relatively warm cloud-top temperatures is seen to the northwest of the downburst echo. [Adapted from Fujita (1978).]

difficult at best, and Fujita never ventured a hypothesis on many of these issues. Another topic left untouched was defining the characteristic time and space scales associated with bow echoes. The examples he presents suggest that the more severe bow echoes typically range in size from about 40 to 120 km and often have lifetimes of several hours. However, bow-shaped systems are observed over a much wider range of scales as well. Finally, he did not characterize the synoptic or mesoscale environments within which such systems are likely to develop.

While research during the 1980s was able to clarify many of the forecasting issues associated with bow echoes, further progress on understanding the kinematic features of bow echoes did not really commence until the early 1990s, when the advent of the Weather Surveillance Radar-1988 Doppler (WSR-88D) network and advancements in computer modeling offered a new opportunity to investigate these phenomena. Perhaps not surprisingly, these more recent studies have confirmed almost all the inferences made by Fujita, as we will now review.

3. Further observational studies

Observational studies during the 1980s and 1990s have continued to clarify the radar-observed characteristics of bow echoes, especially emphasizing features that might signal their development and offer more lead time in the forecasting of the accompanying severe winds or tornadoes. Przybylinski and Gery (1983) and Przybylinski and DeCaire (1985) documented a wide range of radar-echo configurations associated with severe bow echoes, and noted that, "the development of a strong low-level reflectivity gradient near the leading edge of the concave-shaped echo, and the displacement of the maximum echo top over or ahead of the strong low-level reflectivity gradient" were common characteristics as a convective line developed into a bow-shaped system.

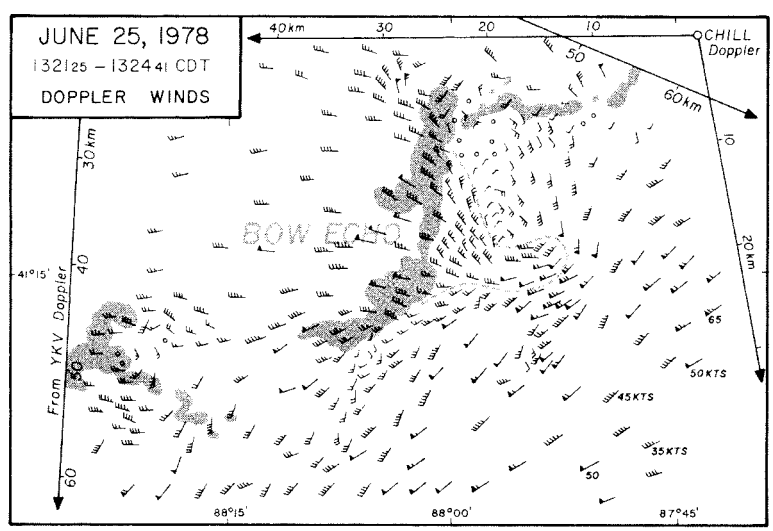

FIG. 10. Dual-Doppler winds on 3.5°C scan surface of the Yorkville, Illinois, (YKV) radar between 1321 and 1325 CDT 25 Jun 1978. The AGL height of the Doppler beam in the high-wind areas is 3.0–3.5 km. [From Fujita (1981).]

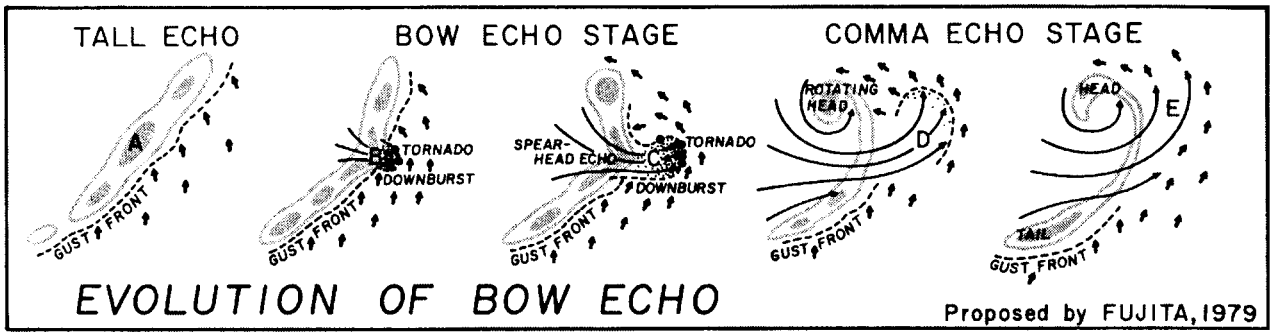

FIG. 11. Revised model of the evolution of bow echo. Bow echo in this new model is produced by a downburst thunderstorm as it snowballs, or cascades, down to the ground. This model is contrary to Fujita's (1978) first thought, "bow echo produces downbursts." [From Fujita (1979).]

These studies were also the first to emphasize that the presence of a "weak echo channel" on the back side of the bow "may signify the presence of downburst winds and possible downburst-induced tornadoes" (Przybylinski and Gery 1983). Later studies further suggested that the weak echo channel signified the loca-

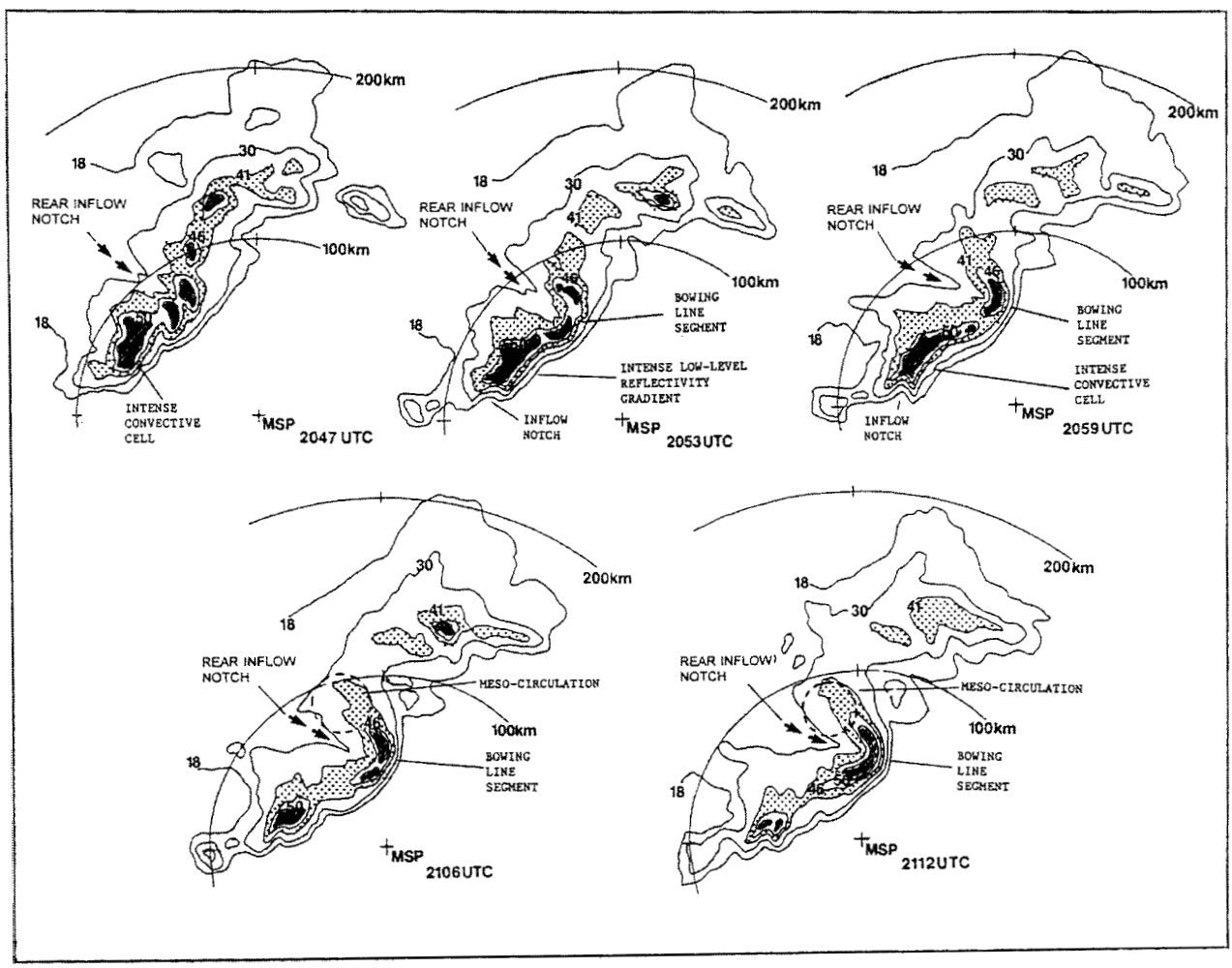

FIG. 12. Radar analysis of the central Minnesota derecho between 2047 and 2112 UTC from Minneapolis–St. Paul, MN (MSP). Reflectivity contours are 18, 30, 41, and 46 dBZ. Shaded region represents reflectivity values greater than 50 dBZ [From Przybylinski (1995).]

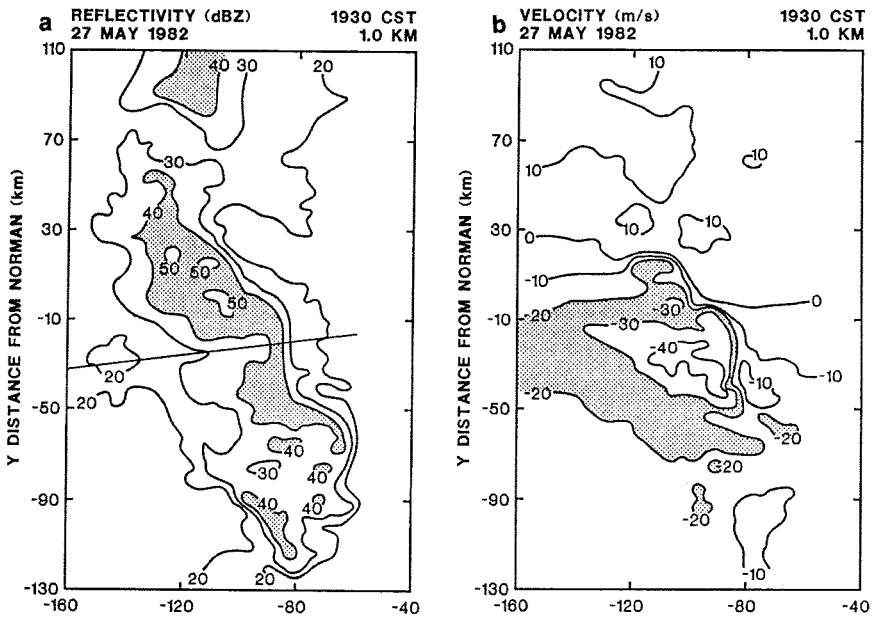

FIG. 13. Norman, OK, single-Doppler analysis of (a) reflectivity (dBZ) and (b) low-resolution velocity (m s^{-1}) for 1930 CST 28 May 1982, at 1 km AGL. [From Burgess and Smull (1990).]

tion of a rear-inflow jet (e.g., Smull and Houze 1985, 1987), which feeds dry, higher momentum air into the downdraft, enhancing the strength of the resulting outflow at the surface through vertical momentum transport and increased evaporation. This association between the "weak echo channel" and a rear-inflow jet has led more recently to the identification of this feature as a "rear-inflow notch" (e.g., Przybylinski 1995). Figure 12 highlights many of these attributes for a bow echo observed in central Minnesota on 19–20 July 1983.

Przybylinski and DeCaire (1985) also emphasized that while a bow echo is generally organized on a scale larger than a single convective cell, individual severe cells, sometimes supercellular, may be contained within the larger-scale structure (e.g., note the intense convective cell with the tight reflectivity gradient and hooklike appendage at the southern end of the bow echo in Fig. 12). However, the frequent observation of bow echoes without apparent supercells suggests that supercell processes are not crucial to the existence of bow echoes.

Doppler observations of bow echoes during the 1980s were scarce but, when available, tended to confirm Fujita's inferences concerning their kinematic structure. Burgess and Smull (1990) document a case that produced damaging winds over a wide swath of central Oklahoma on 27 May 1982. The radar reflectivity field (Fig. 13a) depicts an 80-km-long bow-shaped segment of a larger convective line with a reflectivity minimum noted behind the apex of the bow. The ground-relative winds at about 1.0 km above ground level (AGL) (Fig. 13b) indicate a greater than 40 m s^{-1} rear-inflow jet collocated with this reflectivity notch. Strong flow toward the rear of the system is apparent north and south of this jet feature, indicating the presence of cyclonic and anticyclonic vertical vorticity at the northern and southern ends of the bow system, respectively. Jorgensen and Smull (1993) used airborne Doppler radar to document a bow echo that developed along the dryline in Texas, further confirming the existence of a rear-inflow jet at the apex and vortices at the ends of the bow. Schmidt and Cotton (1989) document a bow-echo case in which one cell was dominant during much of the system's life, having many supercell charac-

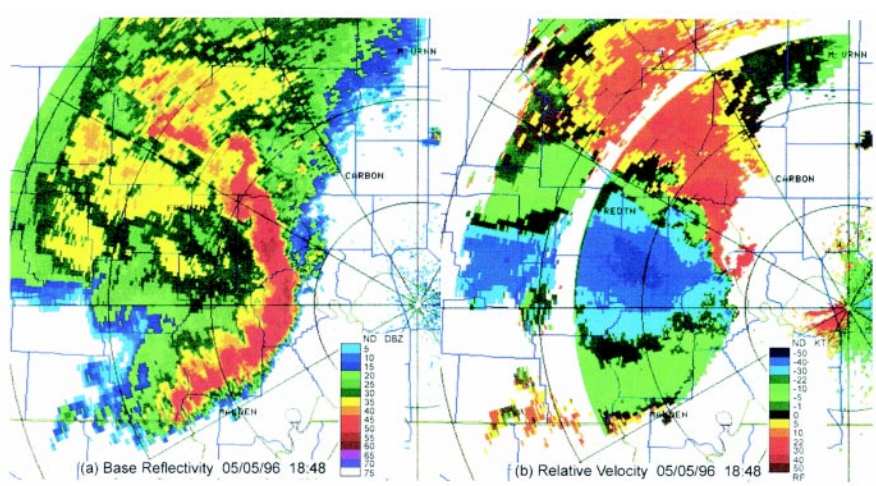

FIG. 14. (a) Base reflectivity and (b) relative velocity from the Paducah WSR-88D radar at 1848 UTC for 5 May 1996. Velocities are presented relative to a storm motion of 33 kt from 280° (R. W. Przybylinski 2000, personal communication).

teristics. The overall structure of the system, however, suggested an organization on a scale larger than that for this individual cell.

The advent of WSR-88D radar during the 1990s has allowed forecasters to monitor the kinematic characteristics (at least from a single-Doppler perspective) of bow echoes while they are occurring. An example is shown in Fig. 14 from the 5 May 1996 case near Paducah, Kentucky, which depicts a large bow-shaped convective system, with two smaller-scale bows embedded within the larger circulation. The Doppler winds clearly depict a large rear-inflow jet behind the core of the system, with weak anticyclonic shear to the south of the bow and stronger cyclonic shear evident on the northern end of the bow. Additionally, the smaller embedded bows each have their own localized rear-inflow jets with associated rotational features on the ends. This event emphasizes that a range of bow-echo scales can exist, sometimes side by side, in the same basic environment. A vertical cross section of reflectivity taken through the core of the bow (Fig. 15a) depicts strong, upright convective cells at the leading edge, with a weaker stratiform region extending rearward. A storm-relative velocity cross section (Fig. 15b) depicts front-to-rear ascending flow through the convective cells and extending aloft within the anvil, with a strong rear-inflow jet beneath the front-to-rear flow at midlevels. These features are remarkably similar to those included in Fujita's schematic cross section based on the 4 July 1977 bow echo, presented in Fig. 6.

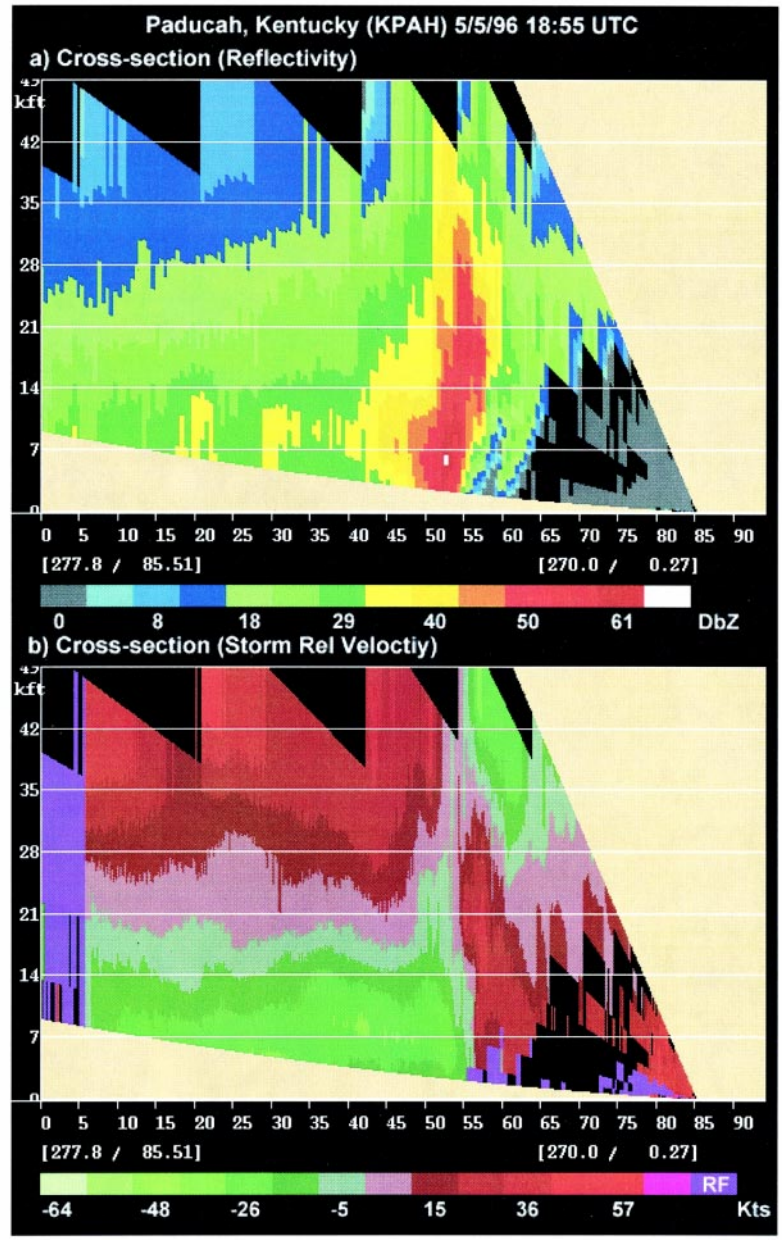

FIG. 15. Vertical cross sections of (a) reflectivity and (b) storm-relative velocity at 1854 UTC for the Paducah, KY, bow echo, as also depicted in Fig. 14. The vertical cross sections are taken at a 277° heading from KPAH. Velocities are presented relative to a storm motion of 20 kts from 277° (R. W. Przybylinski 2000, personal communication).

Doppler radar has also offered the opportunity to identify new radar features that may prove useful for forecasting the onset of severe downburst winds in bow echoes. One potential feature is the midaltitude radial convergence (MARC) signature (Fig. 16) (Schmocker et al. 1996), which is defined as a region of concentrated radial convergence at midlevels in a storm (usually from 3 to 9 km in height). MARC signatures are considered significant if a velocity difference of 25–50 m s^{-1} is observed within a 2–6-km-wide region. Such signatures have been observed 10–30 min before the onset of damaging surface winds. As shown in Fig. 16a, a MARC signature is hypothesized to represent the transition region between the intense front-to-rear ascending updraft current and the rear-inflow jet.

The association between bow echoes and tornadoes has also strengthened since Fujita's initial studies. Przybylinski et al. (1996) and Funk et al. (1996a) de-

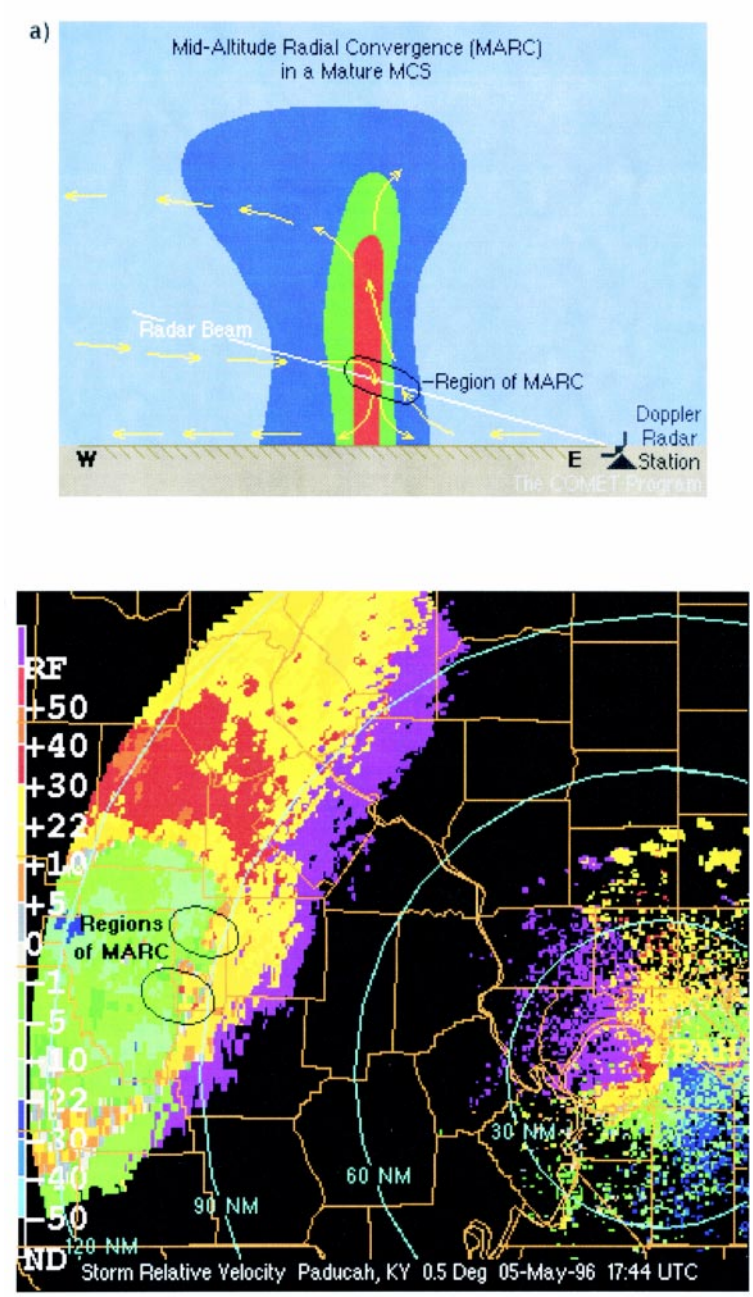

FIG. 16. Schematic representation of a MARC signature associated with downburst-producing convective systems (COMET/UCAR 1999).

scribe a squall line with embedded bow echoes that passed through Illinois, Missouri, Indiana, and Kentucky during the early morning hours of 15 April 1994. This system produced widespread severe surface winds as well as several weak (F0–F1), short-track (about 4 mi) tornadoes along the leading edge of the apex of the bow. A longer-track (25 mi) tornado was also documented, associated with a particularly intense cell [possibly a high precipitation (HP) supercell; e.g., Moller et al. (1994)] embedded within the larger bow-echo structure. Wakimoto (1983), Smith and Partacz (1985), Przybylinski (1988), Funk et al. (1996b), Prost and Gerard (1997), and Pence et al. (1998) describe additional bow echo cases that produced stronger (F2–F4) tornadoes associated with the northern comma head of the bow. For the Wakimoto (1983) case, a strong, anticyclonic tornado was observed north of the apex of the bow. An explanation for the apparent preponderance of tornadoes with bow echoes is as yet forthcoming.

Johns and Hirt (1987) contributed significantly to our understanding of the environments conducive to the development of bow echoes through a climatological study of derechos, which constitute the larger mesoscale convective systems within which bow echoes are often embedded. An example of the extent and longevity of a derecho event is presented in Fig. 17. In this case a squall line produced damaging wind over a swath hundreds of kilometers wide and 1000 km long over 18 h. During the period of May–August for the years 1980–83, Johns and Hirt identified 70 such cases in the United States, most of which occurred in the upper Midwest. More recent climatological studies by Bentley and Mote (1998) and Evans and Doswell (2000, manuscript submitted to *Wea. Forecasting*) identify a similar corridor of derecho development in the upper Midwest, as well as additional corridors along an axis from Kansas through Oklahoma and Texas, and also in the southeast.

Johns and Hirt (1987) identify two basic patterns of radar cells associated with a derecho (Fig. 18). The first pattern (referred to as a progressive derecho) consists of a single bowed segment of convective cells that often develops just on the cool side of a weak stationary front. The bowed feature moves parallel to the front. The second pattern (referred to as a serial derecho) consists of a longer squall line that has evolved into a series of bow echoes or LEWPs that propagate along the squall line.

Johns and Hirt found that the most significant attributes of the derecho environment were the extreme

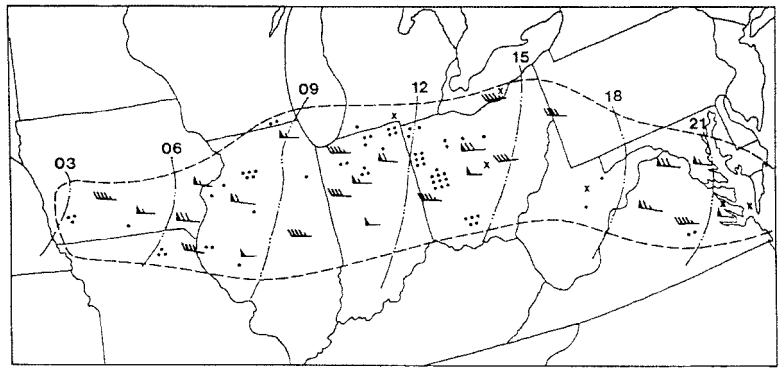

FIG. 17. Area affected by the convective windstorm of 5 Jul 1980 (dashed line). Three-hourly squall-line positions are indicated in UTC (from 0300 5 Jul to 2100 5 Jul). Officially measured convective gusts are indicated by wind barbs (full barb signifies 5 m s^{-1}, flag signifies 25 m s^{-1}). Personal injuries (67) are indicated by dots, and each death (six) is shown by an "x." [From Johns and Hirt (1987).]

amounts of convective instability and low-level moisture. Surface dewpoints were commonly greater than 20°C and the average lifted index was –9°C. In addition, wind strengths in the low- to midtroposphere were greater than that for other types of severe weather outbreaks. The average 500-mb winds were estimated to be 21 m s^{-1}, with the average 700-mb winds at 17 m s^{-1}. As seen in Fig. 19, the instability and shear magnitudes associated with the bow echoes studied by Fujita in 1978 (e.g., Figs. 3 and 7) fall well within this range of derecho environments. More recent studies by Evans (1998), Bentley et al. (1998), and Evans and Doswell (2000, manuscript submitted to *Wea. Forecasting*) further confirm the range of environments associated with derechoes identified in the earlier study.

The most common synoptic pattern associated with derechoes is that described by Johns (1982, 1984) for severe weather outbreaks in northwesterly flow. Over 80% of the 70 events studied by Johns and Hirt (1987) began along or to the north of a weak east-to-west-oriented quasi-stationary frontal boundary and then moved along the boundary (as in the progressive bow echo in Fig. 18). Possible reasons for this association include the enhanced low-level convergence along the zone for triggering convective events, the enhanced instability that might be realized owing to the deepening of the moist layer along the zone, and the enhanced low-level vertical wind shear that would also be generated along such zones (i.e., such generation would be consistent with thermal wind–type arguments, which require the existence of vertical

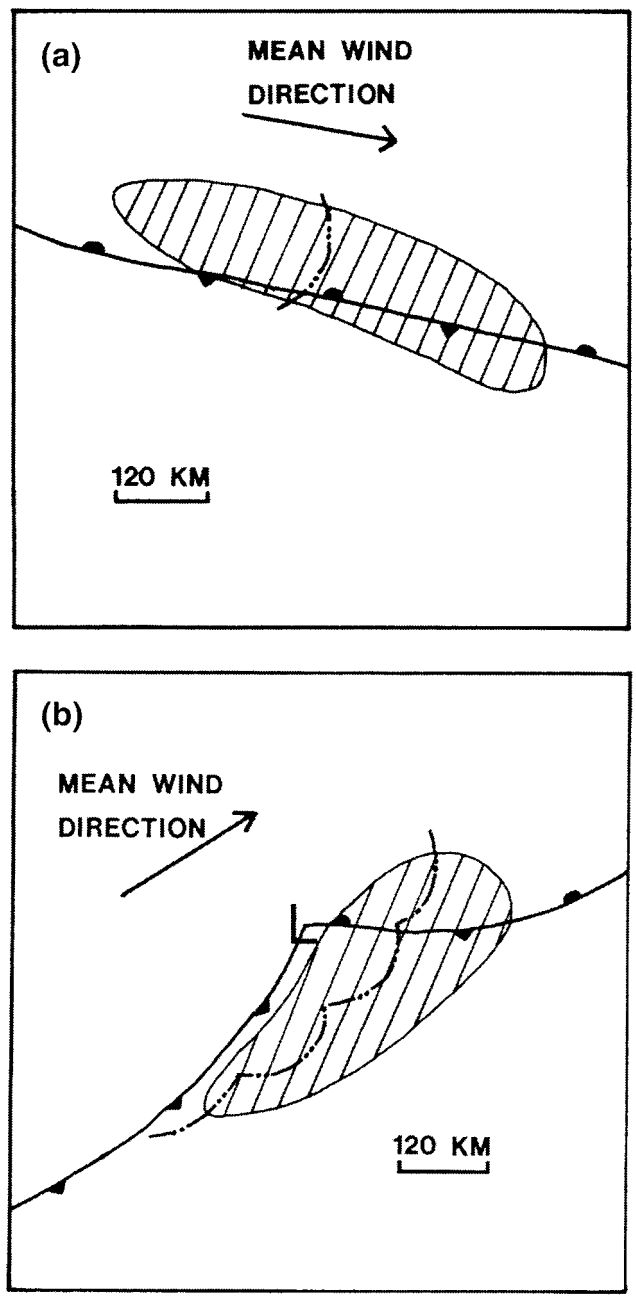

FIG. 18. Schematic representation of features associated with (a) progressive and (b) serial derechoes near the midpoint of their lifetimes. The total area affected by these derechoes is indicated by the hatching. The frontal and squall-line symbols are conventional. [From Johns and Hirt (1987).]

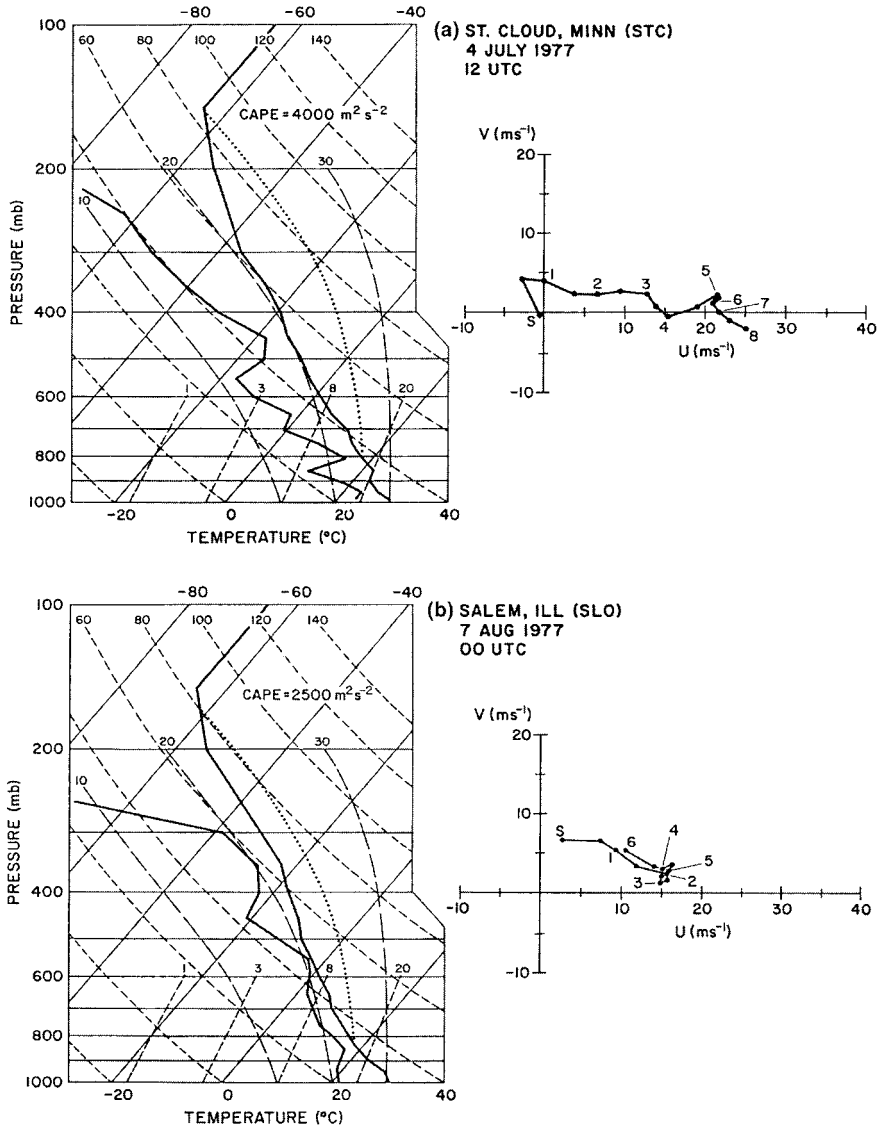

FIG. 19. Estimated thermodynamic and vertical wind shear conditions for the (a) 4 Jul 1977 bow echo, based on the St. Cloud, MN (STC), 1200 UTC sounding, and (b) 7 Aug 1977 bow echo, based on the Salem, IL (SLO), 1200 UTC sounding, as described by Fujita (1978). The thick dotted line on the skew *T* represents an estimated parcel ascent based on the surface observations just ahead of the convective system. The numbers on the hodograph indicate heights in km AGL, with dots spaced every 500 m, starting at the surface (S).

wind shear in association with horizontal gradients in temperature). Further discussions of the relationship between bow echoes and synoptic-scale patterns can be found in Johns and Doswell (1992) and Johns (1993).

Recent observational studies suggest that, although generally not as severe as in midlatitudes, bow-echo-type systems occur in tropical environments as well. Jorgensen et al. (1997) document a bow echo that occurred on 22 February 1993 during the Tropical Ocean Global Atmosphere Coupled Ocean–Atmosphere Response Experiment (TOGA COARE). The environment of this system was characterized by convective available potential energy (CAPE) of about 1440 J Kg^{-1} and a vertical wind shear of 13 m s^{-1} between the surface and 850 mb, which is not quite as strong as for many midlatitude systems, but is strong for tropical environments. The convective system evolves from a symmetric line segment to a bow-shaped segment with a rear-inflow notch and cyclonic vortex on its northern end over a 3-h period, much as described for midlatitude bow echoes. A severe bow echo was also recently documented in Hawaii (Businger et al. 1998).

While the emphasis of these bow-echo studies has been on severe wind-producing systems, it is now becoming recognized that the lifecycle of these systems, as first described by Fujita, represents the generic evolution of a much wider range of nonsevere convective systems as well. Houze et al. (1989) suggested that mature mesoscale convective systems (MCSs) could generally be classified as either symmetric or asymmetric, based on the configuration of radar echoes (Fig. 20). However, more recent observational studies have documented that, rather than representing distinct types of MCSs, such systems tend to evolve from a symmetric to asymmetric configuration during the course of their lifetime (e.g., Loehrer and Johnson 1995; Scott and Rutledge 1995). Similar to Fujita's descriptions of severe bow echoes, mirror-image midlevel vortices are often evident at the ends of the system at early times, with a dominant cyclonic midlevel vortex evident behind the northern end of the system at later times. The 5 May case depicted in Fig. 14 represents an example of what would be classified as an asymmetric MCS. In some cases, the cy-

clonic vortex associated with an asymmetric MCS lives long enough to become dynamically balanced (e.g., Davis and Weisman 1994). Such features have been referred to as mesoscale convective vortices, and have sometimes been observed to last for several days, serving as a trigger for further convective outbreaks (e.g., Bartels and Maddox 1991; Fritsch et al. 1994; Menard and Fritsch 1989). Understanding the initial source of such mesoscale vortices and the evolution to a predominant cyclonic vortex has been the topic of numerous observational and numerical studies over the past decade, as will be described below.

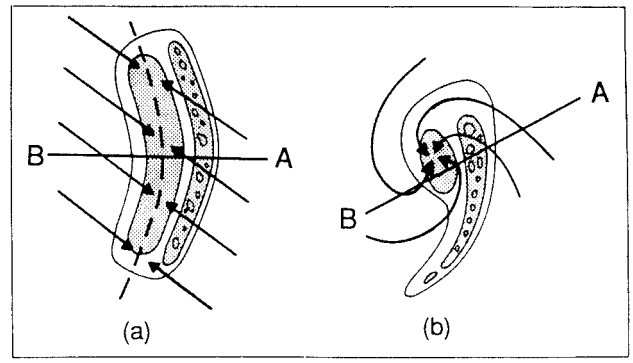

FIG. 20. Schematic of symmetric and asymmetric convective systems. [From Houze et al. (1989).]

4. Recent numerical and dynamical studies

Over the past two decades, numerical models capable of representing air motions on the scale of convective storms have become available and have been invaluable tools in our attempts to understand the dynamics of a variety of convective systems and their relationship to the environment within which they evolve. For instance, early modeling studies concentrated on the relatively short-term (2-h) evolution of isolated convection, and readily reproduced the basic dynamical hierarchy of ordinary versus supercellular convection for increasing magnitudes of environmental vertical wind shear (e.g., Weisman and Klemp 1982, 1984, 1986). Other modeling studies identified the unique dynamics associated with quasi-two-dimensional convective systems such as squall lines (e.g., Thorpe et al. 1982; Rotunno et al. 1988; Weisman et al. 1988). However, it has only been within the last decade or so that computer technology has advanced to the point that simulations could be attempted for the larger time and space scales necessary to represent the life cycle of bow echoes and other large, three-dimensional convective systems. Such simulations have also been able to replicate many of the characteristics of bow echoes and suggest, again, that a unique set of dynamical processes may be responsible for their unusual strength and longevity.

The tendency for a convective cell to evolve into a bow-shaped system of cells for certain environments was first documented in several of the early modeling studies (e.g., Weisman and Klemp 1986). Fundamentally, an updraft produces rain that falls and evaporates, thereby producing a pool of cold air that spreads along the ground. This spreading cold pool produces convergence and lifting along its leading edge that can then trigger new cells. However, rather than a cold pool producing a complete circle of new cells around the initial storm, cells are favored along a bow-shaped arc oriented perpendicular to the vertical wind shear vector. The ability to trigger new cells along this arc increases dramatically as the amount of vertical wind shear increases, and also increases if the wind shear is confined to the lowest 2–3 km AGL.

An explanation for this behavior is offered by Rotunno et al. (1988, hereafter RKW), who found that the best conditions for triggering cells along a spreading cold pool occur when the horizontal vorticity generated by the buoyancy gradient at the edge of the cold pool is matched by the opposing horizontal vorticity inherent in the ambient low-level vertical wind shear. In this situation, a vertical jet of air is created at the leading edge of the cold air that produces deeper lifting than if the shear were not present. This mechanism may, on its own, help explain the strength and longevity of some of the observed convective systems that have been labeled as bow echoes. However, more recent simulations suggest that a unique dynamical structure may evolve within some of these systems that is not explained by these simple relationships.

An example of such a feature occurs in a squall-line simulation presented by Weisman et al. (1988, hereafter WKR). The environmental conditions for this case include a CAPE value of 2400 J kg^{-1} and a unidirectional vertical wind shear of 25 m s^{-1} over the lowest 2.5 km AGL, oriented perpendicular to the squall line. These environmental conditions produce a strong, long-lived, quasi-two-dimensional squall line for which the vertical wind shear is nearly balanced with the system-generated cold pool (as described by RKW). Between 220 and 300 min into the simulation (Fig. 21), however, a 50 km-long bow-shaped segment of cells has developed in the southern portion of the

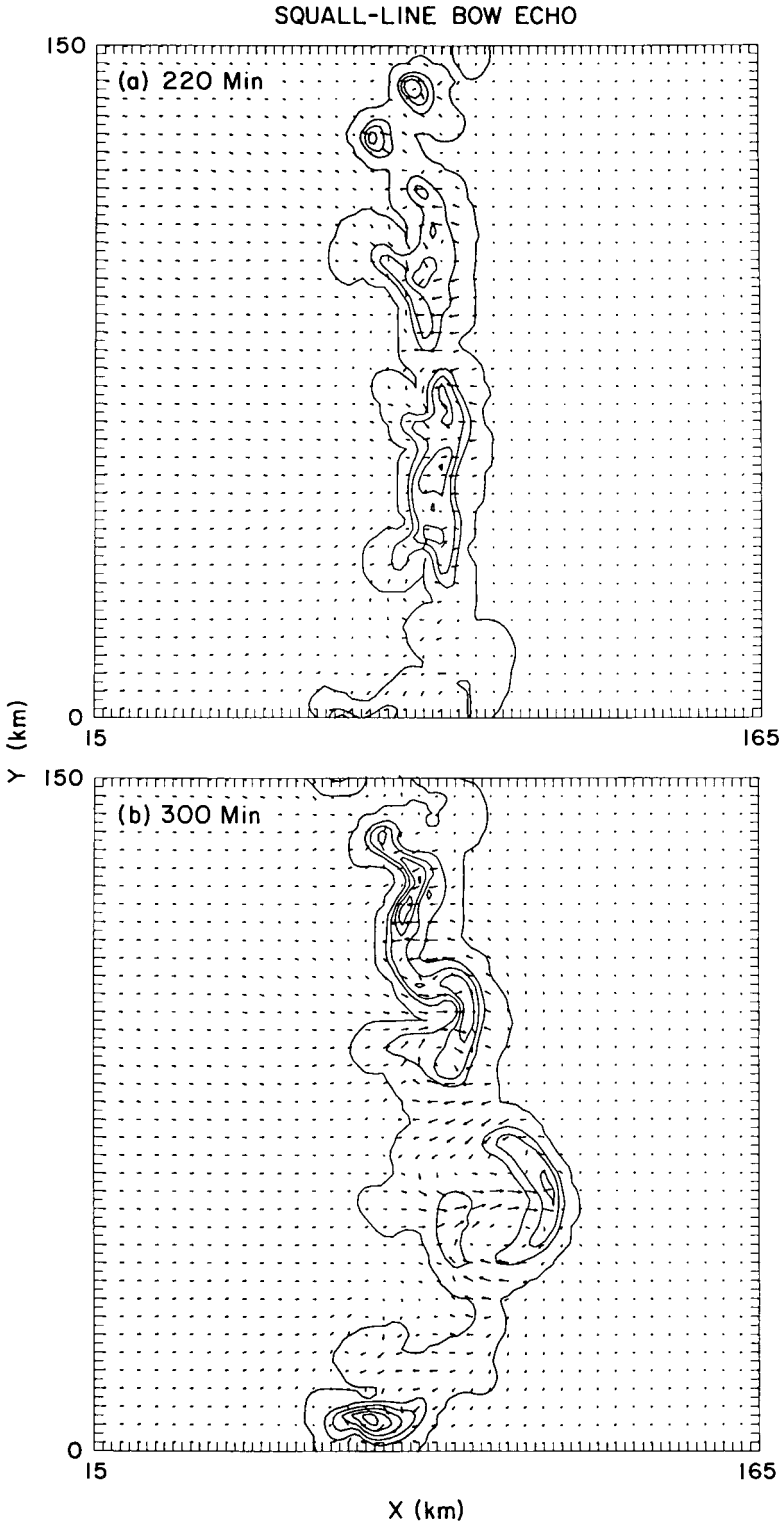

FIG. 21. Horizontal cross sections of system-relative flow and rainwater contours at 2.5 km AGL at 300 min for a squall-line simulation using an environmental vertical wind shear of 25 m s^{-1} over the lowest 2.5 km AGL. A domain speed of U = 22.5 m s^{-1} has been subtracted from the flow vectors. Vectors are plotted at every other grid point (a distance of two grid lengths represents 25 m s^{-1}). The rainwater field is contoured using a 2 g kg^{-1} interval. Only a 150 km by 150 km portion of the entire domain is shown. [Adapted from Weisman (1993).]

domain, with cyclonic and anticyclonic eddies apparent on the northern and southern ends of this line segment, respectively [referred to as line-end or book-end vortices; e.g., Weisman (1993) and Skamarock et al. (1994)]. A strong rear-inflow jet develops behind the center of this bow segment, intensifying to greater than 20 m s^{-1} over the ambient flow at this level. This structure remains coherent for an additional hour, with a smaller bowed segment developing north of the original feature. This smaller bow echo, however, does not retain its structure for as long a period of time.

Through an extensive set of environmental sensitivity experiments, Weisman (1993) documented that the strongest, most coherent bow echoes (e.g., those with an elevated rear-inflow jet and well-defined line-end vortices) occurred primarily in environments of large instability (e.g., CAPEs greater than 2000 J kg^{-1}) and moderate to strong low-level vertical wind shear (e.g., at least 15–20 m s^{-1} of shear over the lowest 2.5–5.0 km AGL). These conditions are quite similar to the environments identified as conducive to derecho formation (e.g., Johns and Hirt 1987). Bow echoes were especially favored in the simulations when the shear was confined to the lowest 2.5 km AGL, as deeper-shear environments tended to produce more isolated supercells. Bow-shaped convective systems with strong surface winds were also produced for weaker shears as well, but such systems were characterized by descending rear-inflow jets and were generally weaker.

Skamarock et al. (1994) and Weisman and Davis (1998) extended these results to finite lines of convective cells, for both weakly and strongly sheared environments, and, furthermore, clarified the role of Coriolis forcing in promoting the development of a dominant cyclonic vortex over time. Figure 22 summarizes these results for two simulations, with and without Coriolis forcing, initiated with five convective cells along a line

150 km in length in an environment with moderate CAPE (2200 J kg^{-1}) and strong low-level vertical wind shear (20 m s^{-1} over the lowest 2.5 km AGL, with constant winds above). In both cases, a line of strong convective cells has become established by 3 h. For the non-Coriolis case (Figs. 22a–c), this line becomes significantly bow shaped between 3 and 6 h, with strong mirror-image cyclonic and anticyclonic midlevel vortices developing at midlevels behind the northern and southern ends of the system, respectively. With Coriolis forcing added (Figs. 22d–f), the northern cyclonic line-end vortex strengthens over time, while the southern anticyclonic vortex weakens, leading to a highly asymmetric system configuration by 6 h. The strengthening of the northern cyclonic vortex was directly related to the midlevel convergence of planetary rotation.

Figures 22d–f also demonstrate that a range of bow-echo scales can be produced within the same convective system, very similar to the observations of the Paducah bow-echo case from 5 May 1996 (Fig. 14). Weisman and Davis documented that the tendency to

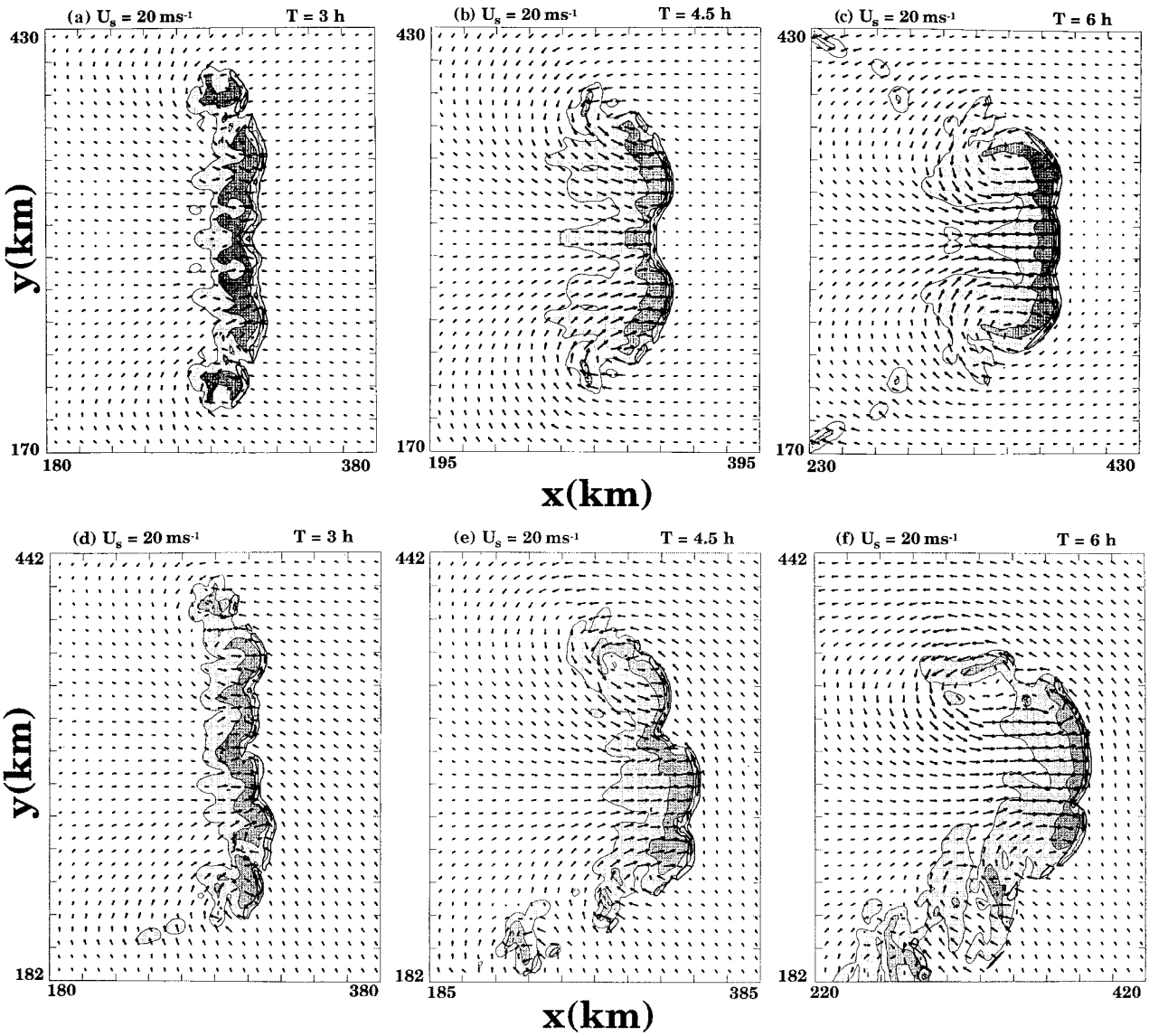

FIG. 22. Horizontal cross sections of system-relative flow, rainwater mixing ratio, and vertical velocity at 2 km AGL for the U_S = 20 m s^{-1} 2.5 km shear: (a–c) non-Coriolis and (d–f) Coriolis simulations at 3, 4.5, and 6 h, respectively. Vectors are presented every four grid points (8 km), with a vector length of 8 km equal to a wind magnitude of 20 m s^{-1}. The rainwater is contoured for magnitudes greater than 1 g kg^{-1} (lightly shaded) and magnitudes greater than 3 g kg^{-1} (darkly shaded). The vertical velocity is contoured at 5 m s^{-1} intervals, with the zero contours omitted. A domain speed of u_m = 18.5 m s^{-1} has been subtracted from the flow field. Tick marks are spaced 20 km apart. [Adapted from Weisman and Davis (1998).]

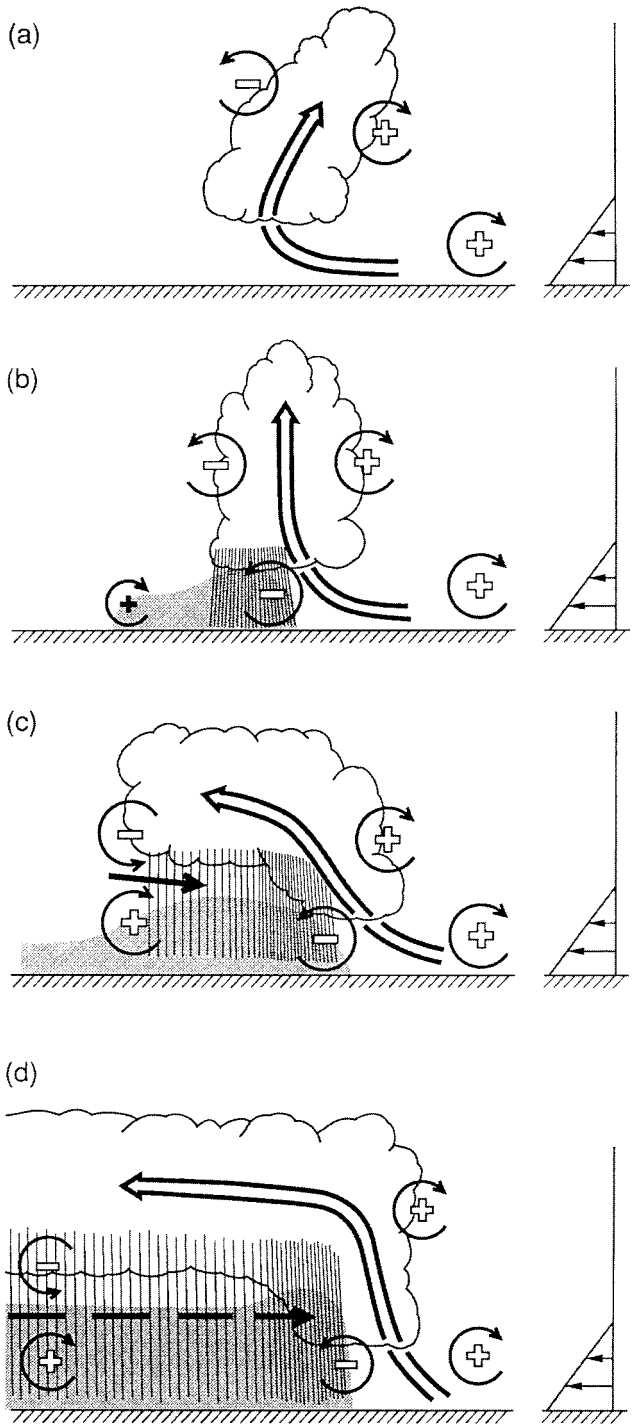

FIG. 23. Four stages in the evolution of an idealized bow echo developing in a strongly sheared, large-CAPE environment. The updraft current is denoted by the thick, double-lined flow vector, with the rear-inflow current in (c) denoted by the thick solid vector. The shading denotes the surface cold pool. The thin, circular arrows depict the most significant sources of horizontal vorticity, which are either associated with the ambient shear or which are generated within the convective system, as described in the text. Regions of lighter or heavier rainfall are indicated by the more sparsely or densely packed vertical lines, respectively. The scalloped line denotes the outline of the cloud. [From Weisman (1993).]

develop such subsystem-scale vortices increased with increasing magnitudes and depth of the ambient vertical wind shear.

Weisman (1993) offered a hypothesis for the development of such systems based on detailed diagnoses of idealized bow-echo simulations. From a two-dimensional perspective (Fig. 23), convective systems tend to evolve from an initially downshear-tilted, to upright, and then upshear-tilted configuration as the convectively generated cold pool strengthens and deepens over time. The speed with which this evolution occurs depends on both the strength of the ambient shear as well as the strength of the convectively generated surface cold pool, with weakly sheared systems evolving through this life cycle over a few hours and more strongly sheared systems taking much longer.

Once the system begins to tilt upshear, a rear-inflow jet is generated in response to the buoyant front-to-rear ascending current aloft and rearward-spreading cold pool at the surface (e.g., Lafore and Moncrieff 1989; Weisman 1992). For most convective systems, this rear-inflow jet descends and spreads along the surface well behind the leading edge of the convection, enhancing the surface outflow but generally weakening the convective system. For the stronger-shear, large-CAPE bow echoes produced in the idealized simulations, however, this rear-inflow jet remains elevated, enhancing the lifting at the leading edge of the system and promoting an even stronger and more long-lived convective system. This configuration of the vertical circulation and elevated rear-inflow jet is quite similar to Fujita's conceptualization of the 4 July 1976 bow echo, as presented in Fig. 6, as well as to the 5 May 1996 case, as presented in Fig. 15.

The development of line-end vortices contributes further to bow-echo severity by focusing and strengthening the midlevel rear-inflow jet between the vortices, thereby enhancing the resultant convective downdrafts and surface outflow. Weisman (1993) traced the initial source of the book-end vortices for strongly sheared systems to the downward tilting of ambient westerly shear within strong cells at the ends of the bow (Fig. 24b), much as described for the development of rotation within the downdrafts associated with splitting supercells (e.g., Klemp 1987). However, Weisman and Davis (1998) clarified that, while the initial source of the line-end vortices could be downward tilting of ambient shear (especially for the stronger-sheared cases), the primary mechanism at later times for all cases was the upward tilting of system-generated easterly shear, associated with the

preferential lifting of the air within the cold pool–warm updraft interface along the leading edge of the bow (Fig. 24a). This easterly shear layer is generated when the cold pool becomes strong enough to promote a system-scale upshear tilt, as depicted in Fig. 23c.

The mature bow-echo configuration of an elevated rear-inflow jet focused between midlevel line-end vortices, along with a steady, intense leading-edge updraft, represents a dynamically unique form of self-sustaining mesoconvective organization. While not all severe, bow-shaped systems become organized to this degree, recognition that such a coherent, long-lived bow echo can exist may help explain some of the more extreme, long-lived severe wind events. Recent successful simulations of a bow-echo-type system observed during TOGA COARE (Trier et al. 1997) also document that the mechanisms identified for bow-echo genesis in midlatitudes apply to the Tropics as well. These results offer more evidence that bow echoes represent a significant form of convective organization.

5. Summary and future research

While much has been learned about bow echoes since Fujita's initial studies, it is particularly remarkable that the basic conceptual model that was presented in 1978 (Fig. 2) has stood the test of time. Indeed, Fujita's observations and insights have carried far beyond their intended use for identifying downburst-producing systems. The basic evolution of a convective line from a symmetric to an asymmetric configuration, with mirror-image line-end vortices evolving to a dominant cyclonic vortex over time, is now recognized as a fundamental mode of convective organization and evolution for severe and nonsevere systems alike. Still, there is much we do not yet understand about such systems.

From the dynamical perspective, one intriguing unresolved issue is the factors that control the scale of such systems. Is the production of severe weather dependent on the scale of the event? Fujita never defined a characteristic scale for bow echoes, although the severe wind-producing cases that he documented ranged from 40 to roughly 120 km in length. However, observations show that bow-shaped systems can exist at scales ranging from a single cell to several hundred kilometers. Even the idealized numerical simulations produce a range of scale for bow-echo-type features, sometimes all within the same mesoscale convective system (e.g., Figs. 22d–f).

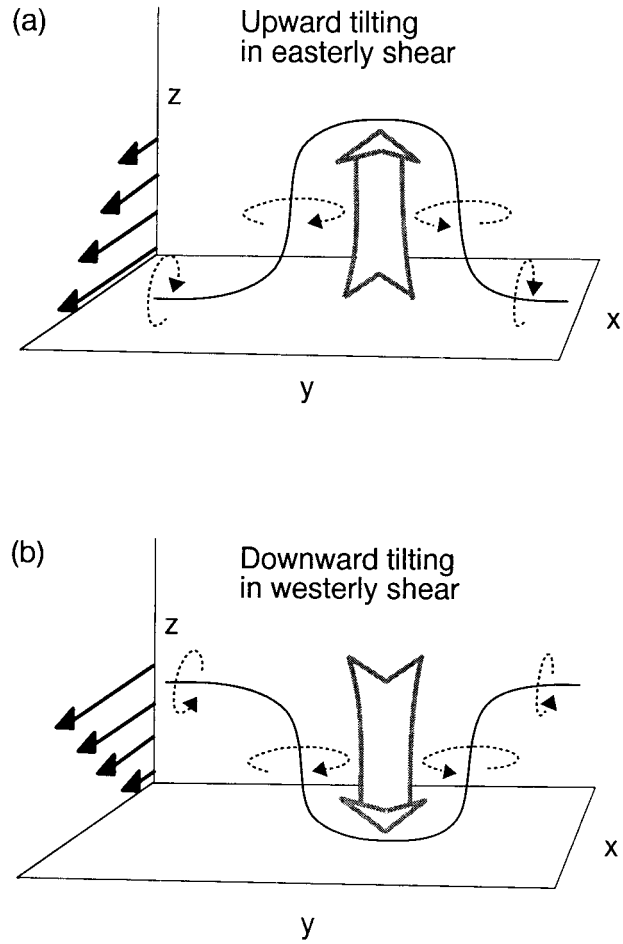

FIG. 24. Schematic of vertical vorticity generation through vortex tilting within finite convective lines and bow echoes. For (a) easterly shear, ascending motion within the central core of a line or bow echo pushes the vortex lines up, resulting in cyclonic rotation on the north end and anticyclonic rotation on the south end of the system. Localized descent in (b) westerly shear produces the same vertical vorticity pattern. [From Weisman and Davis (1998).]

Also, as suggested in these simulations, Coriolis forcing is not necessary for bow-echo generation. Thus, there is no obvious dynamical scale, such as a Rossby radius of deformation, to determine the system's scale. One could argue that the scale is simply controlled by the length of the initial convective line. However, Skamarock et al. (1994) found that, for a given ambient shear, the final scale of the convective system was largely independent of initial line length. The bow-shaped segments embedded within the larger convective line in the Weisman and Davis (1998) simulations originate over a range of scales (e.g., Figs. 22d–f), but the smaller systems tend to congeal over time to perhaps a preferred scale in the

40–80-km range. One possibility is that the scale is selected somewhat based on the ability of the vortices along the line to interact favorably with each other, by strengthening the resulting rear-inflow jet, which affects the lifting at the leading edge of the system, etc. Resolution of these issues, however, must await further study.

Most of the arguments that have been put forth to explain the development of severe winds within bow echoes depend on the development of a strong, deep cold pool and associated mesohigh, which accelerates the surface flow. However, some severe bow echoes have occurred at night in the presence of a stable nocturnal boundary layer that does not as readily support the generation of the strong surface cold pool. A possible example of such an event is the 15 July 1995 event in upper New York State mentioned in the introduction. A similar nighttime convective high wind event is documented and simulated by Bernardet and Cotton (1998). Are the mechanisms for bow-echo genesis and maintenance different for nocturnal versus daytime scenarios?

Another important unresolved issue is the relationship between bow echoes and tornadoes. A particularly intriguing property of bow-echo tornadoes is their tendency to occur primarily from the apex of the bow northward. What are the system-scale circulation features that promote such a preference? On some occasions, low-level circulations that develop along the leading edge of a bow echo are observed to grow in scale and eventually merge with the cyclonic line-end vortices. What is the nature of this interaction? Interestingly, some of the above attributes seem to be reflected in the idealized asymmetric bow-echo simulation presented in Figs. 22d–f, with smaller-scale cyclonic circulations along the leading edge of the system occurring primarily north of the apex of the system, and with some of these circulations eventually merging with the primary northern, cyclonic line-end vortex. A study is currently under way to analyze the generation and evolution of these low-level circulation centers within such simulations.

Issuing appropriate severe weather warnings for bow-echo tornadoes is especially problematic. While supercells and associated tornadoes can be embedded within a bow echo, more often than not, there is no readily identifiable supercell signatures or midlevel mesocyclone preceding such tornadoes. Instead, the rotation usually appears first near the ground, with very little lead time before tornado formation (e.g., Trapp et al. 1999). The relationship between midlevel mesocyclones associated with supercell updrafts and tornadoes and the midlevel line-end vortices that are located behind the active leading-line convection and above the surface cold pool, in general, needs to be clarified (e.g., Funk et al. 1996a). Can current WSR-88D algorithms be modified to more readily distinguish between these two types of features?

Numerical studies of bow echoes to date have only considered highly idealized environments, characterized by horizontally homogeneous initial states. However, bow echoes commonly form in the vicinity of significant surface boundaries and other mesoscale features that could significantly affect system evolution and severe weather production (e.g., Johns and Hirt 1987). Future observational and numerical studies will need to consider more carefully how bow echoes evolve in such complicated mesoscale environments, and to understand how the interactions between bow echoes and preexisting boundaries or convective cells impact the development of severe weather.

Generally, research is still needed to improve the lead times of warnings for all types of severe weather associated with bow echoes. Identifying rear-inflow notches and MARC signatures, etc., are a good start, but studies are also still needed to better understand the factors that control the timing and location of the initiation of bow echoes as well as the factors that control bow-echo demise. What would it take to numerically predict the onset and subsequent evolution of significant bow echoes with enough lead time that the public could respond in a way to mitigate the impacts?

Fujita certainly gave us a big headstart on many of these issues through his careful analyses and insights. But perhaps his most important contributions have been to both motivate the research and forecasting communities as to the potential significance of these systems, as well as to offer us a coherent framework from which to continue our investigations. The value of Fujita's contributions to bow-echo research will be recognized for many years to come.

Acknowledgments. I would like to acknowledge valuable discussions and reviews of this manuscript by Brad Smull, Ron Przybylinski, Jeffrey Trapp, Richard Rotunno, Joseph Klemp, Stan Trier, and one anonymous reviewer. Thanks are also due to Wendy Abshire and Heidi Godskill, for help in preparing several of the figures. Finally, I would especially like to thank Roger Wakimoto, who invited me to write this paper in honor of Dr. Fujita, and who offered many of his personal insights into Fujita's motivations and high character as a scientist and human being.

References

Bartels, D. L., and R. A. Maddox, 1991: Midlevel cyclonic vortices generated by mesoscale convective systems. *Mon. Wea. Rev.,* **119,** 104–118.

Bentley, M. L., and T. L. Mote, 1998: A climatology of derecho-producing mesoscale convective systems in the central and eastern United States, 1986–95. Part I: Temporal and spatial distribution. *Bull. Amer. Meteor. Soc.,* **79,** 2527–2540.

——, ——, and S. F. Byrd, 1998: A synoptic climatology of derecho-producing mesoscale convective systems: 1986–1995. Preprints, *19th Conf. on Severe Local Storms,* Minneapolis, MN, Amer. Meteor. Soc., 5–8.

Bernardet, L. R., and W. R. Cotton, 1998: Multiscale evolution of a derecho-producing mesoscale convective system. *Mon. Wea. Rev.,* **126,** 2991–3015.

Bosart, L. F., W. E. Bracken, A. Seimon, J. W. Cannon, K. D. Lapenta, and J. S. Quinlan, 1998: Large-scale conditions associated with the northwesterly flow intense derecho events of 14–15 July 1995 in the northeastern United States. Preprints, *19th Conf. on Severe Local Storms,* Minneapolis, MN, Amer. Meteor. Soc., 503–506.

Burgess, D. W., and B. F. Smull, 1990: Doppler radar observations of a bow echo associated with a long-track severe windstorm. Preprints, *16th Conf. on Severe Local Storms,* Kananaskis Park, AB, Canada, Amer. Meteor. Soc., 203–208.

Businger, S., T. Birchard Jr., K. Kodama, P. A. Jendrowski, and J. J. Wang, 1998: A bow echo and severe weather associated with a Kona Low in Hawaii. *Wea. Forecasting,* **13,** 576–591.

Cannon, J. W., K. D. Lapenta, J. S. Quinlan, L. F. Bosart, W. E. Bracken, and A. Seimon, 1998: Radar characteristics of the 15 July 1995 northeastern U.S. derecho. Preprints, *19th Conf. on Severe Local Storms,* Minneapolis, MN, Amer. Meteor. Soc., 440–443.

COMET/UCAR, 1999: Mesoscale convective systems: Squall lines and bow echoes. [Available online from http://meted.ucar.edu/convectn/mcs.]

Davis, C. A., and M. L. Weisman, 1994: Balanced dynamics of mesoscale vortices produced in simulated convective systems. *J. Atmos. Sci.,* **51,** 2005–2030.

Evans, J. S., 1998: An examination of observed shear profiles associated with long-lived bow echoes. Preprints, *19th Conf. on Severe Local Storms,* Minneapolis, MN, Amer. Meteor. Soc., 30–33.

Forbes, G. S., and R. M. Wakimoto, 1983: A concentrated outbreak of tornadoes, downbursts and microbursts, and implications regarding vortex classification. *Mon. Wea. Rev.,* **111,** 220–235.

Fritsch, J. M., J. D. Murphy, and J. S. Kain, 1994: Warm-core vortex amplification over land. *J. Atmos. Sci.,* **51,** 1780–1807.

Fujita, T. T., 1978: Manual of downburst identification for project Nimrod. Satellite and Mesometeorology Research Paper 156, Dept. of Geophysical Sciences, University of Chicago, 104 pp. [NTIS PB-286048.]

——, 1979: Objective, operation, and results of Project NIMROD. Preprints, *11th Conf. on Severe Local Storms,* Kansas City, MO, Amer. Meteor. Soc., 259–266.

——, 1981: Tornadoes and downbursts in the context of generalized planetary scales. *J. Atmos. Sci.,* **38,** 1511–1524.

——, and H. R. Byers, 1977: Spearhead echo and downburst in the crash of an airliner. *Mon. Wea. Rev.,* **105,** 129–146.

Funk, T. W., K. E. Darmofal, J. D. Kirkpatrick, M. T. Shields, R. W. Przybylinski, Y.-J. Lin, G. K. Schmocker, and T. J. Shea, 1996a: Storm reflectivity and mesocyclone evolution associated with the 15 April 1994 derecho. Part II: Storm structure and evolution over Kentucky and southern Indiana. Preprints, *18th Conf. on Severe Local Storms,* San Francisco, CA, Amer. Meteor. Soc., 516–520.

——, B. F. Smull, and J. D. Ammerman, 1996b: Structure and evolution of an intense bow echo embedded within a heavy rain producing MCS over Missouri. Preprints, *18th Conf. on Severe Local Storms,* San Francisco, CA, Amer. Meteor. Soc., 521–526.

Hamilton, R. E., 1970: Use of detailed intensity radar data in mesoscale surface analysis of the 4 July 1969 storm in Ohio. Preprints, *14th Conf. on Radar Meteorology,* Tucson, AZ, Amer. Meteor. Soc., 339–342.

Hinrichs, G., 1888: Tornadoes and derechos. *Amer. Meteor. J.,* **5,** 306–317, 341–349.

Houze, R. A., S. A. Rutledge, M. I. Biggerstaff, and B. F. Smull, 1989: Interpretation of Doppler weather radar displays of midlatitude mesoscale convective systems. *Bull. Amer. Meteor. Soc.,* **70,** 608–619.

Johns, R. H., 1982: A synoptic climatology of northwest flow severe weather outbreaks. Part 1: Nature and significance. *Mon. Wea. Rev.,* **110,** 1653–1663.

——, 1984: A synoptic climatology of northwest-flow severe weather outbreaks. Part 2: Meteorological parameters and synoptic patterns. *Mon. Wea. Rev.,* **112,** 449–464.

——, 1993: Meteorological conditions associated with bow echo development in convective storms. *Wea. Forecasting,* **8,** 294–299.

——, and W. D. Hirt, 1987: Derechos: Widespread convectively induced wind-storms. *Wea. Forecasting,* **2,** 32–49.

——, and C. A Doswell III, 1992: Severe local storm forecasting. *Wea. Forecasting,* **7,** 588–612.

Jorgensen, D. P., and B. F. Smull, 1993: Mesovortex circulations seen by airborne Doppler radar within a bow-echo mesoscale convective system. *Bull. Amer. Meteor. Soc.,* **74,** 2146–2157.

——, M. A. LeMone, and S. B. Trier, 1997: Structure and evolution of the 22 February 1993 TOGA COARE squall line: Aircraft observations of precipitation, circulation, and surface energy fluxes. *J. Atmos. Sci.,* **54,** 1961–1985.

Klemp, J. B., 1987: Dynamics of tornadic thunderstorms. *Annu. Rev. Fluid Mech.,* **19,** 369–402.

Lafore, J., and M. W. Moncrieff, 1989: A numerical investigation of the organization and interaction of the convective and stratiform regions of tropical squall lines. *J. Atmos. Sci.,* **46,** 521–544.

Loehrer, S. M., and R. H. Johnson, 1995: Surface pressure and precipitation life cycle characteristics of PRE-STORM mesoscale convective systems. *Mon. Wea. Rev.,* **123,** 600–621.

McCarthy, D., 1996: Mesoscale aspects of the New York State derecho July 15, 1995. Preprints, *15th Conf. on Weather Analysis and Forecasting,* Norfolk, VA, Amer. Meteor. Soc., 370–373.

Menard, R. D., and J. M. Fritsch, 1989: A mesoscale convective complex-generated inertially stable warm core vortex. *Mon. Wea. Rev.,* **117,** 1237–1260.

Moller, A. R., C. A. Doswell III, M. P. Foster, and G. R. Woodall, 1994: The operational recognition of supercell thunderstorm environments and storm structures. *Wea. Forecasting,* **9,** 327–347.

Nolen, R. H., 1959: A radar pattern associated with tornadoes. *Bull. Amer. Meteor. Soc.,* **40,** 277–279.

Pence, K. J., J. T. Bradshaw, and M. W. Rose, 1998: The central Alabama tornadoes of 6 March 1996. Preprints, *19th Conf. on Severe Local Storms,* Minneapolis, MN, Amer. Meteor. Soc., 147–154.

Prost, R. L., and A. E. Gerard, 1997: "Bookend vortex"–induced tornadoes along the Natchez Trace. *Wea. Forecasting,* **12,** 572–580.

Przybylinski, R. W., 1988: Radar signatures with the 10 March 1986 tornado outbreak over central Indiana. Preprints, *15th Conf. on Severe Local Storms,* Baltimore, MD, Amer. Meteor. Soc., 253–256.

——, 1995: The bow echo. Observations, numerical simulations, and severe weather detection methods. *Wea. Forecasting,* **10,** 203–218.

——, and W. J. Gery, 1983: The reliability of the bow echo as an important severe weather signature. Preprints, *13th Conf. on Severe Local Storms,* Tulsa, OK, Amer. Meteor. Soc., 270–273.

——, and D. M. DeCaire, 1985: Radar signatures associated with the derecho, a type of mesoscale convective system. Preprints, *14th Conf. on Severe Local Storms,* Indianapolis, IN, Amer. Meteor. Soc., 228–231.

——, and Coauthors, 1996: Storm reflectivity and mesocyclone evolution associated with the 15 April 1994 derecho. Part I: Storm evolution over Missouri and Illinois. Preprints, *18th Conf. on Severe Local Storms,* San Franscisco, CA, Amer. Meteor. Soc., 509–515.

Rasch, W., and R. L. van Ess, 1998: Case study of a strong bow echo in North Dakota on 17 May 1996. Preprints, *19th Conf. on Severe Local Storms,* Minneapolis, MN, Amer. Meteor. Soc., 484–485.

Rinehart, R. E., and E. T. Garvey, 1978: Three-dimensional storm motion determined by conventional weather radar. *Nature,* **273,** 287–289.

Rotunno, R., J. B. Klemp, and M. L. Weisman, 1988: A theory for strong, long-lived squall lines. *J. Atmos. Sci.,* **45,** 463–485.

Schmidt, J. M., and W. R. Cotton, 1989: A high plains squall line associated with severe surface winds. *J. Atmos. Sci.,* **46,** 281–302.

Schmocker, G. K., R. W. Przybylinski, and Y. J. Lin, 1996: Forecasting the initial onset of damaging downburst winds associated with a mesoscale convective system (MCS) using the mid-altitude radial convergence (MARC) signature. Preprints, *15th Conf. on Weather Analysis and Forecasting,* Norfolk, VA, Amer. Meteor. Soc., 306–311.

Scott, J. D., and S. A. Rutledge, 1995: Doppler radar observations of an asymmetric mesoscale convective system and associated vortex couplet. *Mon. Wea. Rev.,* **123,** 3437–3457.

Skamarock, W. C., M. L. Weisman, and J. B. Klemp, 1994: Three-dimensional evolution of simulated long-lived squall lines. *J. Atmos. Sci.,* **51,** 2563–2584.

Smith, B. E., and J. W. Partacz, 1985: Bow-echo induced tornado at Minneapolis on 26 April 1984. Preprints, *14th Conf. on Severe Local Storms,* Indianapolis, IN, Amer. Meteor. Soc., 81–84.

Smull, B. F., and R. A. Houze Jr., 1985: A midlatitude squall line with a trailing region of stratiform rain: Radar and satellite observations. *Mon. Wea. Rev.,* **113,** 117–133.

——, and ——, 1987: Rear inflow in squall lines with trailing stratiform precipitation. *Mon. Wea. Rev.,* **115,** 2869–2889.

Spoden, P. J., C. N. Jones, J. Keysor, and M. Lamm, 1998: Observations of flow structure and mesoscale circulations associated with the 5 May 1996 asymmetric derecho in the lower Ohio Valley. Preprints, *19th Conf. on Severe Local Storms,* Minneapolis, MN, Amer. Meteor. Soc., 514–517.

Thorpe, A. J., M. J. Miller, and M. W. Moncrieff, 1982: Two-dimensional convection in non-constant shear: A model of mid-latitude squall lines. *Quart. J. Meteor. Soc.,* **108,** 739–762.

Trapp, R. J., E. D. Mitchell, G. A. Tipton, D. W. Effertz, A. I. Watson, D. L. Andra Jr., and M. A. Magsig, 1999: Descending and non-descending tornadic vortex signatures detected by WSR-88Ds. *Wea. Forecasting,* **14,** 625–639.

Trier, S. B., W. C. Skamarock, and M. A. LeMone, 1997: Structure and evolution of the 22 February 1993 TOGA COARE squall line: Organization mechanisms inferred from numerical simulation. *J. Atmos. Sci.,* **54,** 386–407.

Tuttle, J. D., and G. B. Foote, 1990: Determination of the boundary-layer airflow from a single Doppler radar. *J. Atmos. Oceanic Technol.,* **7,** 218–232.

Wakimoto, R. M., 1983: The West Bend, Wisconsin storm of 4 April 1981: A problem in operational meteorology. *J. Climate Appl. Meteor.,* **22,** 181–189.

Weisman, M. L., 1992: The role of convectively generated rear-inflow jets in the evolution of long-lived mesoconvective systems. *J. Atmos. Sci.,* **49,** 1826–1847.

——, 1993: The genesis of severe, long-lived bow-echoes. *J. Atmos. Sci.,* **50,** 645–670.

——, and J. B. Klemp, 1982: The dependence of numerically simulated convective storms on vertical wind shear and buoyancy. *Mon. Wea. Rev.,* **110,** 504–520.

——, and ——, 1984: The structure and classification of numerically simulated convective storms in directionally varying wind shears. *Mon. Wea. Rev.,* **112,** 2479–2498.

——, and ——, 1986: Characteristics of isolated convective storms. *Mesoscale Meteorology and Forecasting,* P. S. Ray, Ed., Amer. Meteor. Soc., 331–358.

——, and C. Davis, 1998: Mechanisms for the generation of mesoscale vortices within quasi-linear convective systems. *J. Atmos. Sci.,* **55,** 2603–2622.

——, ——, and R. Rotunno, 1988: Structure and evolution of numerically simulated squall lines. *J. Atmos. Sci.,* **45,** 1990–2013.

Wilson, J. W., and R. M. Wakimoto, 2001. The discovery of the downburst: T. T. Fujita's contribution. *Bull. Amer. Meteor. Soc.,* **82,** 49–62.